

## THERMODYNAMICS OF DECONFINED QCD AT SMALL AND LARGE CHEMICAL POTENTIAL

ANDREAS IPP \*

*Institut für Theoretische Physik, Technische Universität Wien  
Wiedner Hauptstr. 8-10/136, A-1040 Vienna, Austria  
E-mail: ipp@hep.itp.tuwien.ac.at*

We present large  $N_f$  QCD/QED as a test bed for improved pressure calculations, show how to apply the hints obtained on optimized renormalization scales at large  $N_f$  to finite  $N_f = 2$ , and compare the results to recent lattice data.

### 1. Introduction

In the deconfined phase of QCD, strict perturbative calculations of thermodynamic potentials show poor convergence when approaching the phase transition. There have been a number of attempts to overcome this problem by reorganization or partial resummation of the perturbative expansions, like HTL perturbation theory<sup>1</sup> or  $\Phi$ -derivable approximations for 2PI skeletons<sup>2</sup>, but so far independent verification of these models was only possible through lattice simulations<sup>3</sup>. It is therefore instructive to consider the exactly solvable special case of large number of flavors (large  $N_f$ ), in which the improvements above can be tested<sup>4</sup>. The large  $N_f$  limit can furthermore be easily extended to finite chemical potential<sup>5</sup>. Also, effects relevant to full QCD, like the anomalous specific heat at low temperatures, can be readily studied in the large- $N_f$  limit<sup>6,7</sup>.

### 2. Large $N_f$

The limit of large number of flavors is formed by sending  $N_f$  to infinity, while keeping the combination  $g^2 N_f$  as well as  $N_c$  of the order of  $O(1)$ . The diagrams contributing to the free energy are at leading order (LO) only the fermion loop, while at next-to-leading order (NLO) an infinite

---

\*Work supported by the Austrian Science Foundation FWF, project no. 16387-N08.

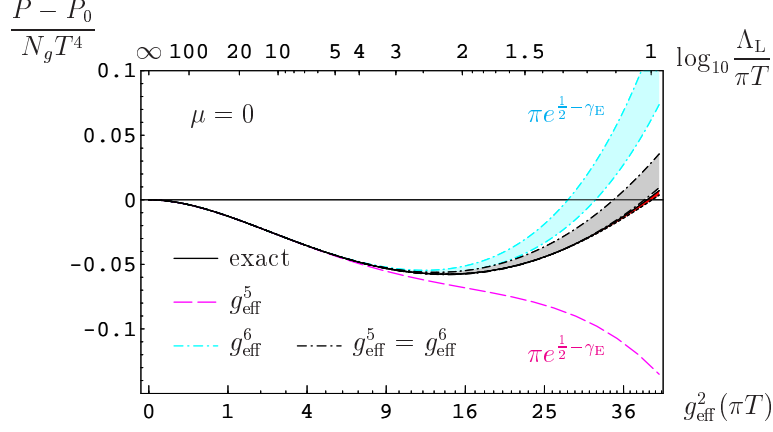


Figure 1. Exact result for the interaction pressure at zero chemical potential as a function of  $g_{\text{eff}}^2(\bar{\mu}_{\text{MS}} = \pi T)$ . The dashed line is the perturbative result, evaluated with renormalization scale  $\bar{\mu}_{\text{MS}} = \bar{\mu}_{\text{FAC}}$ ; the light band includes the numerically determined coefficient to order  $g_{\text{eff}}^6$  (with its estimated error) also at  $\bar{\mu}_{\text{FAC}}$ . The result marked “ $g_{\text{eff}}^5 = g_{\text{eff}}^6$ ” corresponds to choosing  $\bar{\mu}_{\text{MS}}$  such that the order- $g_{\text{eff}}^6$  coefficient vanishes and retaining all higher-order terms contained in the plasmon term  $\propto m_E^3$ .

number of ring diagrams consisting of a boson loop with any number of fermion loop insertions have to be summed up<sup>4</sup>. We can treat massless QCD and ultrarelativistic QED at the same time by defining an effective coupling as  $g_{\text{eff}}^2 \equiv g^2 N_f / 2$  for QCD and  $g_{\text{eff}}^2 \equiv e^2 N_f$  for QED. Large  $N_f$  contains a Landau pole of the order of  $\Lambda_L \sim \mu \exp(6\pi^2 / g_{\text{eff}}^2)$ , but the resulting ambiguity for the thermal pressure at NLO is suppressed by a factor  $(\max(T, \mu) / \Lambda_L)^4$ .

After subtracting off the vacuum part of the ring diagrams and applying Schwinger-Dyson resummation<sup>4</sup>, the NLO thermal pressure is given by

$$\begin{aligned} \frac{P_{\text{NLO}}}{N_g} = & - \int \frac{d^3 q}{(2\pi)^3} \int_0^\infty \frac{dq_0}{\pi} \left[ 2 \left( [n_b + \frac{1}{2}] \text{Im} \ln(q^2 - q_0^2 + \Pi_T + \Pi_{\text{vac}}) \right. \right. \\ & \left. \left. - \frac{1}{2} \text{Im} \ln(q^2 - q_0^2 + \Pi_{\text{vac}}) \right) \right. \\ & \left. + \left( [n_b + \frac{1}{2}] \text{Im} \ln\left(\frac{q^2 - q_0^2 + \Pi_L + \Pi_{\text{vac}}}{q^2 - q_0^2}\right) - \frac{1}{2} \text{Im} \ln\left(\frac{q^2 - q_0^2 + \Pi_{\text{vac}}}{q^2 - q_0^2}\right) \right) \right] \quad (1) \end{aligned}$$

with the bosonic distribution function  $n_b(\omega) = 1/(e^{\omega/T} - 1)$  and the gauge-boson self energy functions  $\Pi_T$  and  $\Pi_L$ . These cannot be given in closed form except for their imaginary parts<sup>8</sup>, but are represented by one-dimensional integrals. We therefore have to evaluate the integrals numerically. Parts proportional to  $n_b$  can be safely integrated in Minkowski

space, but terms without  $n_b$  are potentially logarithmically divergent. We compute them by introducing a Euclidean invariant cutoff<sup>4</sup>.

### 3. Numerical results

Figure 1 shows the numerical result for  $\mu = 0$  as a function of  $g_{\text{eff}}^2(\bar{\mu}_{\text{MS}} = \pi T)$ . For small coupling the coefficients to order  $g_{\text{eff}}^6$  which are not yet known analytically can be extracted numerically<sup>5</sup>. The large renormalization scale dependences of successive perturbative approximations to order  $g_{\text{eff}}^5$  beyond  $g_{\text{eff}}^2 \sim 4$  can be fixed by applying “fastest apparent convergence” (FAC) in the  $m_E^2$  parameter of dimensional reduction. Using  $\bar{\mu}_{\text{MS}} = \bar{\mu}_{\text{FAC}} \equiv \pi e^{1/2-\gamma} T$  we obtain good agreement up to  $g_{\text{eff}}^2 \sim 9$ . The result can be further improved by the procedures explained below Fig. 1.

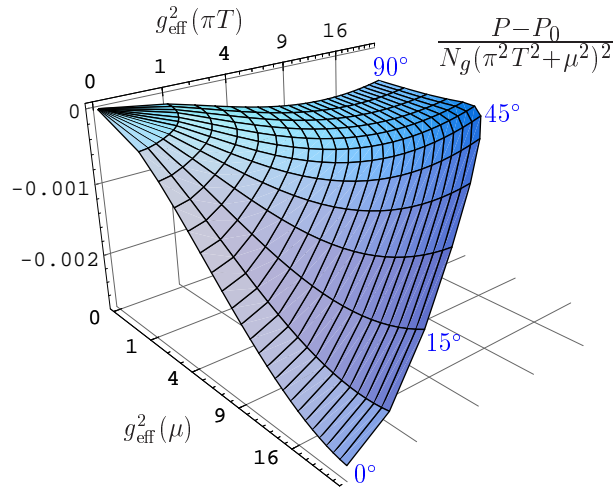


Figure 2. Exact result for the large- $N_f$  interaction pressure  $P - P_0$  normalized to  $N_g(\pi^2 T^2 + \mu^2)^2$  as a function of  $g_{\text{eff}}^2(\bar{\mu}_{\text{MS}})$  with  $\bar{\mu}_{\text{MS}}^2 = \pi^2 T^2 + \mu^2$  and  $\phi = \arctan \frac{\pi T}{\mu}$ .

For non-vanishing chemical potential  $\mu$  we use the fermionic distribution function

$$n_f(k, T, \mu) = \frac{1}{2} \left( \frac{1}{e^{(k-\mu)/T} + 1} + \frac{1}{e^{(k+\mu)/T} + 1} \right) \quad (2)$$

which enters via the gauge boson self-energy expressions  $\Pi_T$  and  $\Pi_L$ . In Fig. 2 we display our exact results for the interaction pressure  $P - P_0 \propto N_f^0$

for the entire  $\mu$ - $T$  plane (but reasonably below the scale Landau pole). The figure shows a kink at  $\phi = 45^\circ$  corresponding to  $\mu = \pi T$  indicating that a simple scaling behavior for the pressure at small chemical potentials would break down at larger chemical potentials<sup>5</sup>.

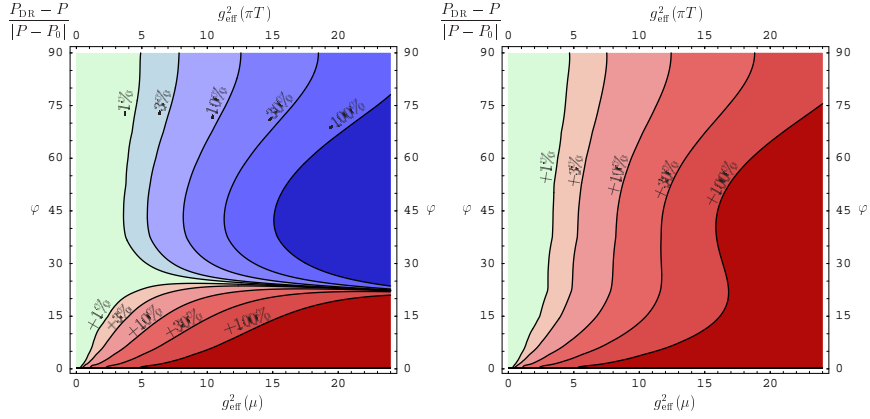


Figure 3. Percentage errors of the perturbative result for the interaction part of the pressure to order  $g_{\text{eff}}^5$  in the large- $N_f$  limit as a function of  $\varphi = \arctan(\pi T/\mu)$  and  $g_{\text{eff}}^2(\bar{\mu}_{\text{MS}})$  at  $\bar{\mu}_{\text{MS}} = \sqrt{\pi^2 T^2 + \mu^2}$  for two choices of  $\bar{\mu}_{\text{MS}}$ : Fastest apparent convergence of  $P$  as well as  $m_E^2$  (FAC-m, left panel), and of  $g_E^2$  (FAC-g, right panel). The brightest area corresponds to an error of less than 1%, the darkest ones to an error of over 100%.

Figure 3 shows a comparison between the perturbative result obtained by dimensional reduction<sup>9</sup> through order  $g^5$  with complete analytic dependence on arbitrary  $T$  and  $\mu$  to the exact result in the large  $N_f$  limit. In the left panel the renormalization scale is  $\bar{\mu}_{\text{MS}} = \bar{\mu}_{\text{MS}}^{\text{FAC-m}}$ . An alternative choice for the renormalization scale is to set  $\bar{\mu}_{\text{MS}}$  such that the  $g_{\text{eff}}^4$  correction in the dimensional reduction coupling parameter  $g_E^2$  is put to zero (FAC-g, right panel). The accuracy of the results is comparable in both cases and decreases slowly with increasing chemical potential, apart from an accidental zero of the error; for  $\varphi \lesssim 18^\circ$ , i.e.  $T \lesssim 0.1\mu$ , the errors eventually start to grow rapidly, marking the breakdown of dimensional reduction. This is precisely the region where non-Fermi-liquid effects lead to anomalous  $T \ln T^{-1}$  terms in the entropy and specific heat<sup>6,7</sup>.

In Fig. 4 we display the FAC optimized results<sup>10</sup> at finite  $N_f = 2$  for the difference  $\Delta P = P(T, \mu) - P(T, 0)$  for various  $\mu/T$  corresponding to recent lattice results<sup>11</sup> assuming  $T_0 \equiv T_c^{\mu=0} = 0.49 \Lambda_{\text{QCD}}$ <sup>12</sup>. At  $T/T_0 = 2$  our FAC-g and FAC-m results exceed the not-yet-continuum-extrapolated

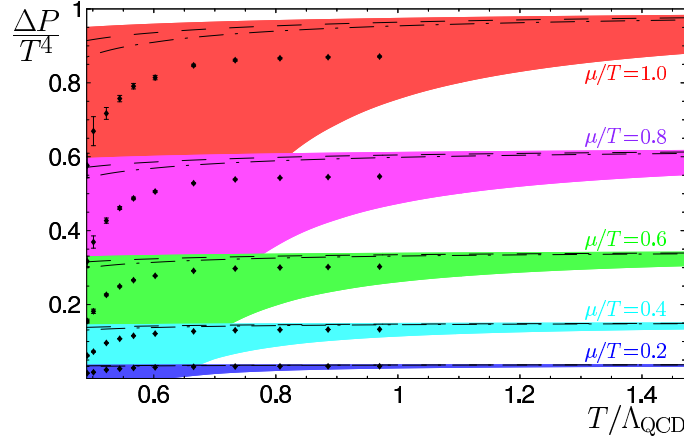


Figure 4. The difference  $\Delta P = P(T, \mu) - P(T, 0)$  divided by  $T^4$  for  $N_f = 2$  using the unexpanded three-loop result from dimensional reduction for  $\mu/T = 0.2, \dots, 1.0$  (bottom to top). Shaded areas correspond to a variation of  $\bar{\mu}_{\text{MS}}$  around the FAC-m choice by a factor of 2; dashed and dash-dotted lines correspond to the FAC-g and FAC-m results, respectively. Also included are recent lattice data (not yet continuum-extrapolated!) assuming  $T_c^{\mu=0} = 0.49 \Lambda_{\text{QCD}}$ .

lattice data consistently by 10.5% and 9%, respectively, which is roughly the expected discretization error<sup>13</sup>.

## References

1. J. O. Andersen, E. Braaten, and M. Strickland, Phys. Rev. Lett. **83** (1999) 2139–2142; R. Baier and K. Redlich, Phys. Rev. Lett. **84** (2000) 2100.
2. J. P. Blaizot, E. Iancu, and A. Rebhan, Phys. Rev. Lett. **83** (1999) 2906–2909; Phys. Rev. **D63** (2001) 065003; A. Peshier, Phys. Rev. **D63** (2001) 105004.
3. G. Boyd *et al.*, Nucl. Phys. **B469** (1996) 419–444; CP-PACS Collaboration, M. Okamoto *et al.*, Phys. Rev. **D60** (1999) 094510.
4. G. D. Moore, JHEP **0210**, 055 (2002); A. Ipp, G. D. Moore, and A. Rebhan, JHEP **0301**, 037 (2003).
5. A. Ipp and A. Rebhan, JHEP **0306**, 032 (2003).
6. A. Ipp, A. Gerhold, and A. Rebhan, Phys. Rev. **D69**, 011901 (2004).
7. A. Gerhold, A. Ipp, and A. Rebhan, hep-ph/0406087; see also contribution in these proceedings.
8. A. Ipp, PhD thesis TU Vienna 2003, hep-ph/0405123.
9. A. Vuorinen, Phys. Rev. **D68**, 054017 (2003).
10. A. Ipp, A. Rebhan and A. Vuorinen, Phys. Rev. D **69**, 077901 (2004).
11. C. R. Allton *et al.*, Phys. Rev. **D68**, 014507 (2003).
12. S. Gupta, Phys. Rev. **D64**, 034507 (2001).
13. F. Karsch, E. Laermann, and A. Peikert, Phys. Lett. **B478**, 447 (2000).